INTERNATIONAL SOCIETY FOR SOIL MECHANICS AND GEOTECHNICAL ENGINEERING

SIMSG ISSMGE

Inertial and spreading load combinations of soil-pile-structure system during liquefaction-induced lateral spreading in centrifuge tests

Combinaisons de charge d'inertie et de propagation sur des systèmes sol-pieu-structure pendant la propagation latérale provoquée par la liquéfaction dans des essais de centrifugeuse

D. Chang, R. W. Boulanger, B. L. Kutter & S. J. Brandenberg
Department of Civil and Environmental Engineering
University of California, Davis, CA 95616, USA
e-mail: ddchang@ucdavis.edu

ABSTRACT

Eight dynamic centrifuge model experiments were performed on the 9-m radius centrifuge at UC Davis to study the combinations of inertial and lateral spreading soil loads on piles in liquefied and laterally spreading ground. Two of the centrifuge models, which are the focus of this paper, consisted of a simple superstructure on a pile group in gently sloping ground. Scaled earthquake motions were applied to each of the models. Time histories of inertia and lateral spreading crust loads on the piles foundation were back calculated from the dense instrumentation arrays. The load transfer mechanism between the nonliquefied crust layer and the pile cap was also compared with results from prior centrifuge tests without superstructures and in different soil profiles (Boulanger et al. 2003, Brandenberg et al. 2004). The resulting insights regarding the loading mechanism of foundations in laterally spreading ground, timing of inertia and spreading crust loads throughout shaking and contribution of cap inertia are summarized.

RÉSUMÉ

Afin d'étudier les combinaisons de charge d'inertie et de propagation latérale du sol sur des pieux dans du sol liquéfié et en état de propagation latérale, huit essais dynamiques ont été effectués sur la centrifugeuse de 9 mètres de rayon de UC Davis. Deux des modèles consistent en une superstructure simple sur un groupe de pieux dans du sol en légère pente. Les modèles ont été soumis à des mouvements sismiques d'amplitude adaptée. En utilisant des mesures provenant de réseaux denses d'instrumentation, des séries temporelles de charges d'inertie et de propagation latérale du sol agissant sur les pieux ont été rétro calculées. Le mécanisme de transfert de charge entre la couche de sol non liquéfiée et la tête de pieu a également été comparé avec les résultats de modèles sans superstructures et avec des profils de sol différents (Boulanger et al. 2003, Brandenberg et al. 2004). Les conclusions concernant le mécanisme de chargement de fondations dans du sol en état de propagation latérale sont résumées ainsi que celles concernant la contribution de l'inertie de la tête et le timing des charges d'inertie et de propagation de la croûte pendant le séisme.

1 INTRODUCTION

The loads imposed on pile foundations by laterally spreading ground due to earthquake-induced liquefaction are a major design consideration for pile-supported structures, where prediction of the loading conditions (e.g., Figure 1) is a complex problem involving consideration of design motions, free field site response, ground deformations, and soil-pile-structure interaction. A better understanding of the mechanisms of inertial and kinematic interactions is needed to improve current design methods for cost-effective foundations that can sustain lateral spreading with an acceptable level of performance (e.g., post-earthquake serviceability or collapse prevention).

Figure 1: Schematic of pile-supported structure in laterally spreading ground.

2 CENTRIFUGE TESTS

A series of eight centrifuge model experiments were performed with scaled earthquake motions in the 9-m radius centrifuge in UC Davis to study the behavior of piles in liquefied and laterally spreading ground. Two of them, namely DDC01 and DDC02, included simple superstructures on pile groups embedded in a gently sloping (4°) soil profile with a clay crust overlying liquefiable loose sand ($D_r \approx 35\%$) overlying dense sand ($D_r \approx 75\%$). Structure period and undrained shear strength of the clay crust were the only differences between the two tests, where the structures, supported on groups of 3 by 2 piles with prototype diameter of 1.17-m, had fixed-base periods of 0.3 s in DDC01 and 0.8 s in DDC02, and the undrained shear strengths of clay were 22 kPa in DDC01 and 33 kPa in DDC02. Figure 2 shows the schematic cross section of centrifuge model DDC02, with a fixed-base structure period of 0.8-s and clay undrained shear strength of 33 kPa.

Details for all the eight centrifuge experiments were summarized in a series of data reports available from the web site for the Center for Geotechnical Modeling at UCD (http://cgm.engr.ucdavis.edu). These data reports include detailed explanations of model construction, data acquisition procedures, data organizational structure, post-earthquake model dissection measurements, and the recorded data (e.g., Chang et al. 2004a,b).
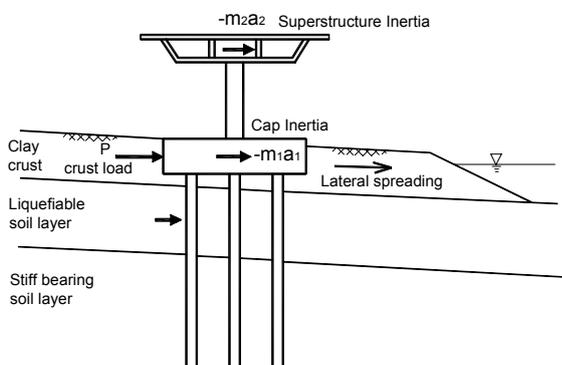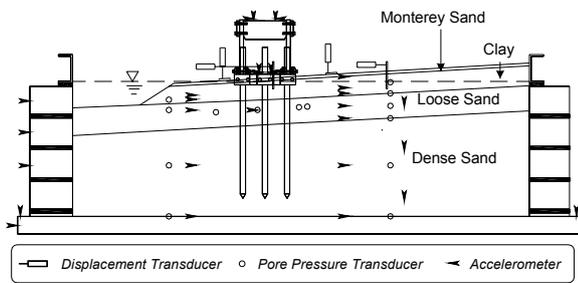
Figure 2: Schematic model layout of test DDC02.

3 TEST OBSERVATIONS

3.1 Back calculation of load components

Time histories of different load components were obtained by processing the over 100 instrument records from each of the centrifuge tests. Additional details including typical time histories can be found in Chang et al. (2005).

Figure 3 shows the lateral loads on the pile cap in lateral spreading ground. The lateral forces on the cap include:

I_1: inertial force from the superstructure mass ($I_1 = -m_1a_1$).
I_2: inertial force from the pile cap mass ($I_2 = -m_2a_2$).
P_{crust}: crust load imposed on the pile cap and pile segments.
V: total shear force measured a little below the pile cap.

From horizontal equilibrium of the pile cap free-body shown in Figure 3, the crust load imposed on the cap could be calculated by the difference between the total shear and inertial forces.

The superstructure inertia I_2 and cap inertia I_1 were obtained by accelerometer recordings, and the total shear V was measured by strain gages on the piles at a small distance below the pile cap. The crust load P_{crust} includes passive force upslope of the pile cap, horizontal friction between base and sides of the pile cap and the crust, and forces on the pile segments between the base of the cap and the strain gages. Theoretical prediction of the crust load components can be found in Boulanger et al. (2003).

For model DDC02 during a large Kobe motion, selected time histories of recorded raw data are plotted in Figure 4, which includes the maximum bending moment and shear force in one pile, the horizontal accelerations of the superstructure mass and the pile cap, the excess pore water pressure in the middle of loose sand layer, and the lateral displacements of the clay crust and the pile cap.

Back-calculated force time histories are shown, along with other representative recordings, in Figure 5, which includes the total shear force (V), the crust load (P_{crust}), the cap inertia, the superstructure inertia, the excess pore pressure ratio (r_u) in the middle of loose sand layer, the lateral displacements of the pile cap relative to the "free field" soil surface, and the base acceleration. Together, the time histories for all earthquakes show the following attributes:

- The shear and bending moments on the piles and the inertial responses all show low-frequency components that reflect the fact that a major load on the piles is from the crust load, which has similar low frequency components.

- The critical cycle that produced the peak total shear and peak bending moment on the piles always occurred during shaking and coincided with transient reductions in r_u in the liquefiable sand.
- The inertia and crust loads were simultaneously at, or near, their respective peaks values at the critical loading cycles (maximum shear), and were acting in-phase.
- The cap inertia was of comparable magnitude and was in phase with the superstructure inertia during the critical loading cycles.
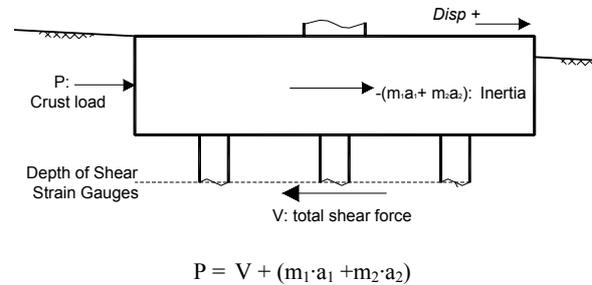

$$P = V + (m_1 \cdot a_1 + m_2 \cdot a_2)$$

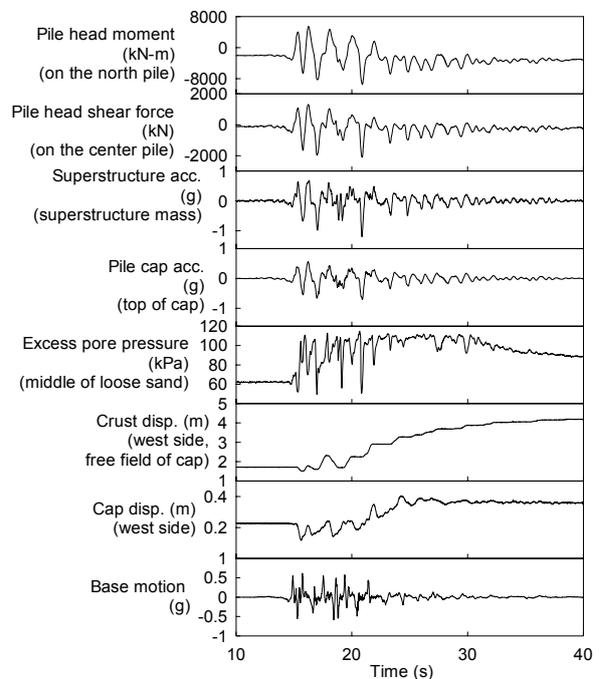Figure 3: Lateral forces acting on the pile cap.

Figure 4: Recorded time histories of DDC02 in a large Kobe motion.

3.2 Phasing of inertial and lateral spreading loads

The crust load was the major driving force on the pile-structure system and it was characterized by low-frequency (long-period) components relative to the base shaking motion (i.e., as a result of liquefaction in the sand beneath the crust). The pile-structure systems were thereby excited primarily in their first mode of vibration with the crust load, cap inertia, and superstructure inertia tending to be in phase at critical cycles. The shorter-period second mode of vibration for the system was relatively weak because it was not excited by the long-period crust load and was also likely more heavily damped by the soil-pile cap interaction. These observations

are consistent with those reported by Tokimatsu (2003) and Tokimatsu et al. (2004), wherein they conclude that if the natural period of the structure is less than that of the ground, then the inertial and kinematic forces are in phase.

Cap inertia was of comparable magnitude with superstructure inertia at the critical loading cycles during shaking for both models. The cap mass can become significant when pile groups must be designed to resist large lateral spreading forces. Figure 6 plots the measured cap accelerations versus superstructure accelerations at the critical loading cycles for different earthquake motions, which shows that cap inertia is not negligible when considering lateral force equilibrium.
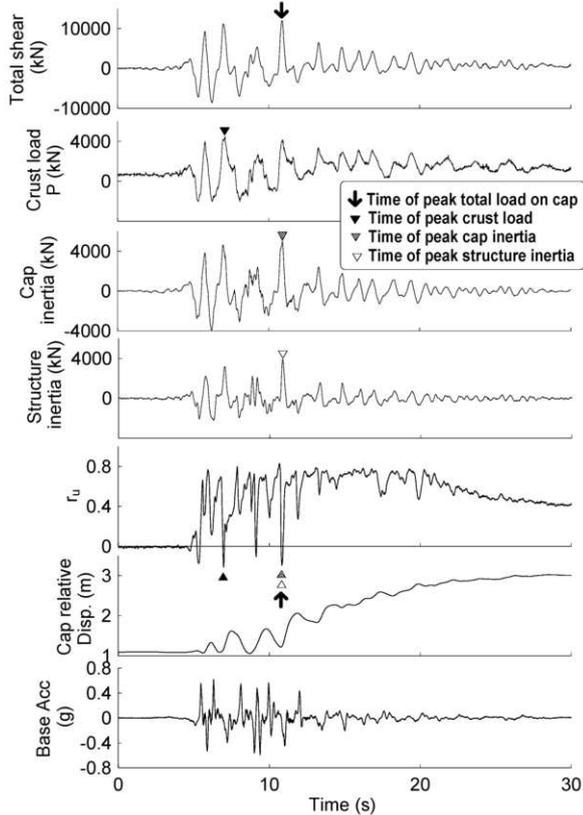

Figure 5: Back-calculated force and recorded time histories of DDC02 in a large Kobe motion.
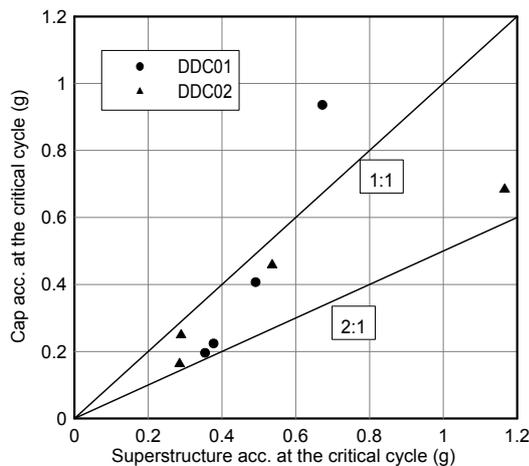

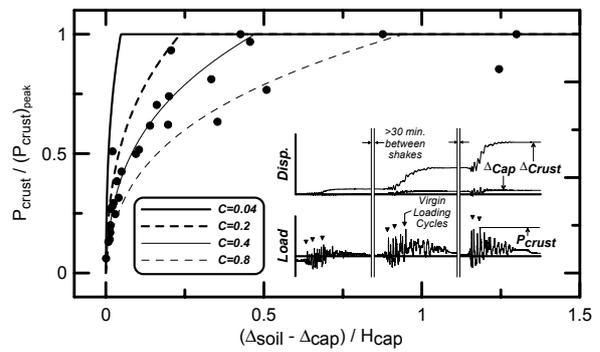Figure 6: Peak pile cap acceleration versus peak superstructure acceleration at critical cycles.

Figure 7: Normalized lateral load from the surface crust versus the relative cap-soil displacement (Brandenberg et al. 2004).

### 3.3   Lateral load transfer from crust to pile cap

The peak lateral load from the clay crust (P_{crust}) in the large Kobe motion was found to be consistent with theoretical expectations for total crust load (Boulanger et al. 2003). However, very large cap-soil relative displacements were required to reach that theoretical peak, as shown by the centrifuge tests results in Figure 7. The relative displacement at which peak crust loads were mobilized in the various centrifuge tests in this study was almost an order of magnitude larger than would be expected based on analogy to static lateral loading relations. This difference is attributed somewhat to effect of cyclic degradation, but mostly to the effect of liquefaction beneath the clay crust which results in the pile cap imposing strains on the clay crust to greater distances away from the cap. These aspects of behavior are described in greater detail in Brandenberg et al. (2004).

4 LOAD COMBINATIONS

The measured crust load $[(P_{crust})_{t=tcr}]$ and inertial force $[(I_1+I_2)_{t=tcr}]$ (sum of superstructure inertia I_1 and cap inertia I_2) at the critical loading cycle (at peak total shear force, t=tcr) were normalized by the peak crust load $[(P_{crust})_{pk}]$ and the peak inertia load $[(I_1+I_2)_{pk}]$ during the same motion, respectively, and plotted against the peak base acceleration of all the earthquake motions for both models in Figure 8(a). Note that the peak crust load and peak inertia load occurred at very nearly the same time in most shaking events, and thus the results in Figure 8(a) show that the measured inertia and crust loads at the critical loading cycle for a given earthquake motion were within 6% to 23% of their own overall peaks during that motion; i.e., the ratio $(I_1+I_2)_{t=tcr}/(I_1+I_2)_{pk}$ was always greater than 94% and the ratio $(P_{crust})_{t=tcr}/(P_{crust})_{pk}$ was greater than 83% in all but one motion. The measured peak total shear at the critical cycle ($V_{t=tcr}$) was subsequently normalized by the sum of the peak crust load and peak inertia load (sum of superstructure and cap inertia loads) during the same motion, and plotted against peak base acceleration for all the motions and both models in Figure 8(b). These results show that directly adding the peak inertia load and peak crust load together (even when they occurred at different times) would produce a close estimation (within 12%) of the peak total shear on the pile cap.
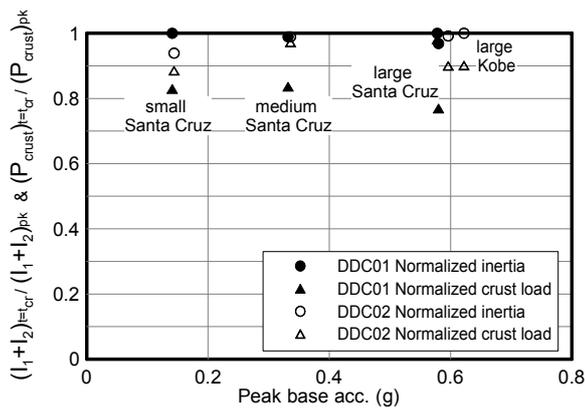
(a) Normalized inertia & crust load
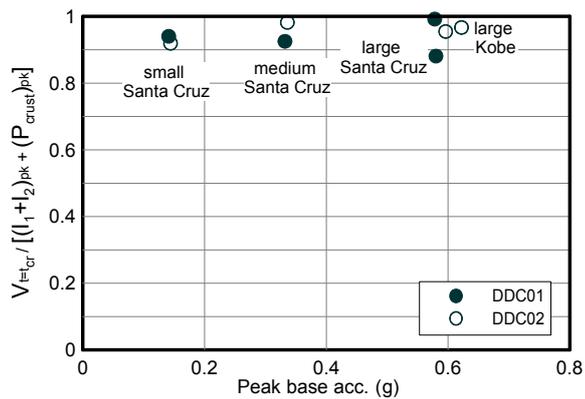
(b) Normalized total shear

Figure 8: Normalized loads versus peak base acceleration.

5 CONCLUDING REMARKS

Two centrifuge models of simple superstructures supported on pile groups embedded in a sloping soil profile with a clay crust overlying liquefiable loose sand over dense sand were shaken with a series of scaled earthquake motions. The nonliquefied crust laterally spreads down slope on top of the liquefiable sand, imposing a large crust load on the pile foundation, which along with the inertial forces from the superstructure mass and pile cap mass, are the main loads on the pile foundation during earthquake shaking and lateral spreading.

The appropriate combinations of crust and inertial loads for design of pile foundations depends on the dominant frequencies of the major driving forces on the foundation relative to the effective fundamental periods of the pile-structure system. In these experiments, the crust load was a major driving force and it was characterized by low-frequency components (i.e., as a result of liquefaction in the sand beneath the crust). The pile-structure system was thereby excited primarily in its first mode of vibration with the crust load, cap inertia, and superstructure inertia tending to be in phase at critical cycles. The peak shear force on the pile foundations could therefore be reasonably estimated as the sum of the peak crust load and the peak inertial load. The fact that liquefaction results in relatively long period crust loads is an important consideration when evaluating whether inertial and lateral spreading loads will likely be in-phase or not.

REFERENCES

Boulanger, R. W., Kutter, B. L., Brandenberg, S. J., Singh, P., and Chang, D. (2003). Pile foundations in liquefied and laterally spreading ground during earthquakes: Centrifuge experiments and analyses. Report UCD/CGM-03/01, Center for Geotechnical Modeling, Univ. of California, Davis, CA.

Brandenberg, S., Boulanger, R., Kutter, B., Wilson, D., and Chang, D. (2004). "Load transfer between pile groups and laterally spreading ground during earthquakes." *13th World Conference on Earthquake Engineering,* Vancouver, Canada, paper No. 1516.

Chang, D., Boulanger, R. W., Kutter, B. L., and Brandenberg, S. J. (2005). "Experimental observations of inertial and lateral spreading loads on pile groups during earthquakes." Geo-Frontiers Conference, Austin, Texas, January.

Chang, D., Brandenberg, S. J., Boulanger, R. W., and Kutter, B. L. (2004a). "Behavior of piles in laterally spreading ground during earthquakes – centrifuge data report for DDC01" Report No. UCD/CGMDR-04/01, Center for Geotechnical Modeling, Department of Civil Engineering, University of California, Davis.

Chang, D., Brandenberg, S. J., Boulanger, R. W., and Kutter, B. L. (2004b). "Behavior of piles in laterally spreading ground during earthquakes – centrifuge data report for DDC02." Report No. UCD/CGMDR-04/02, Center for Geotechnical Modeling, Department of Civil Engineering, University of California, Davis.

Tokimatsu, K. (2003). "Behavior and design of pile foundations subjected to earthquakes." *Twelfth Asian Regional Conference on Soil Mechanics and Geotechnical Engineering,* Japan.

Tokimatsu, K., Suzuki, H., and Sato, M. (2004). "Effects of inertial and kinematic forces on pile stresses in large shaking table tests." *13th World Conference on Earthquake Engineering* Vancouver, Canada, paper No. 1322.